

This article was downloaded by:

On: 14 January 2011

Access details: *Access Details: Free Access*

Publisher *Taylor & Francis*

Informa Ltd Registered in England and Wales Registered Number: 1072954 Registered office: Mortimer House, 37-41 Mortimer Street, London W1T 3JH, UK



Molecular Simulation

Publication details, including instructions for authors and subscription information:

<http://www.informaworld.com/smpp/title~content=t713644482>

Molecular Dynamics/Free Energy Perturbation Studies of the Thermostable V74I Mutant of Ribonuclease HI

Ryuji Tanimura^{ab}; Minoru Saito^a

^a Protein Engineering Research Institute, Suita, Osaka, Japan ^b Basic Research Laboratories, Toray Industries, Inc., Kamakura, Kanagawa, Japan

To cite this Article Tanimura, Ryuji and Saito, Minoru(1996) 'Molecular Dynamics/Free Energy Perturbation Studies of the Thermostable V74I Mutant of Ribonuclease HI', *Molecular Simulation*, 16: 1, 75 — 85

To link to this Article: DOI: 10.1080/08927029608024062

URL: <http://dx.doi.org/10.1080/08927029608024062>

PLEASE SCROLL DOWN FOR ARTICLE

Full terms and conditions of use: <http://www.informaworld.com/terms-and-conditions-of-access.pdf>

This article may be used for research, teaching and private study purposes. Any substantial or systematic reproduction, re-distribution, re-selling, loan or sub-licensing, systematic supply or distribution in any form to anyone is expressly forbidden.

The publisher does not give any warranty express or implied or make any representation that the contents will be complete or accurate or up to date. The accuracy of any instructions, formulae and drug doses should be independently verified with primary sources. The publisher shall not be liable for any loss, actions, claims, proceedings, demand or costs or damages whatsoever or howsoever caused arising directly or indirectly in connection with or arising out of the use of this material.

MOLECULAR DYNAMICS/FREE ENERGY PERTURBATION STUDIES OF THE THERMOSTABLE V74I MUTANT OF RIBONUCLEASE HI

RYUJI TANIMURA¹ and MINORU SAITO*

*Protein Engineering Research Institute
6-2-3 Furuedai, Suita, Osaka, 565 Japan*

(Received November 1994, accepted June 1995)

Recent site-directed mutagenesis and thermodynamic studies have shown that the V74I mutant of *Escherichia coli* ribonuclease HI (RNase HI) is more stable than the wild type protein [Ishikawa *et al.*, *Biochemistry* 32, 6171 (1993)]. In order to clarify the stabilization mechanism of this mutant, we calculated the free energy change due to the mutation Val74→Ile in both the native and denatured states by free energy perturbations based on molecular dynamics (MD) simulations. We carried out inclusive MD simulations for the protein in water; *i.e.*, fully solvated, no artificial constraints applied, and all long-range Coulomb interactions included. We found that the free energy of the mutant increased slightly relative to the wild type, in the native state by 1.60 kcal/mol, and in the denatured state by 2.25 kcal/mol. The unfolding free energy increment of the mutant (0.66 ± 0.19 kcal/mol) was in good agreement with the experimental value (0.6 kcal/mol). The hysteresis error in the free energy calculations, *i.e.*, forward and reverse perturbations, was only ± 0.19 kcal/mol. These results show that the V74I mutant is stabilized relative to the wild type by the increased free energy of the denatured state and not by a decrease in the free energy of the native state as had been proposed earlier based on the mutant X-ray structure. It was found that the stabilization was caused by a loss of solvation energy in the mutant denatured state and not by improved packing interactions inside the native protein.

KEY WORDS: Cavity-filling mutation, free energy perturbation method, thermal stability, particle-particle and particle-cell (PPPC) method, acceptance ratio method (ARM).

1 INTRODUCTION

Proteins are stabilized by various interactions, such as disulfide bonds, helix-dipole interactions, the conformational freedom of glycine and proline residues, and hydrophobic interactions. The hydrophobic interaction is regarded as one of the dominant factors among them stabilizing the interior of a protein [1–6]. The role of the hydrophobic interaction in determining protein stability has been widely studied experimentally by cavity-creating mutations which replace a buried nonpolar side chain in the wild type with a smaller one in the mutants of various proteins, *i.e.* T4

* To whom correspondence should be addressed.

¹Present address: Toray Industries, Inc. Basic Research Laboratories, 1111, Teburo, Kamakura, Kanagawa, 248, Japan.

lysozyme [2, 7–10], the alpha-subunit of tryptophan synthase [11], barnase [4, 5], lambda-repressor protein [12], the gene V protein from bacteriophage f1 [6, 13], and staphylococcal nuclease [3]. Only a few studies have been designed to increase protein stability by cavity-filling mutations introducing bulkier residues into the interior of a protein [14, 15]. In a recent study of *Escherichia coli* ribonuclease HI (RNase HI), the V74I mutant, in which the buried Val74 is replaced with the bulkier Ile residue, was the only mutant which was found to be stabilized relative to the wild type [16], except for mutants replaced with unnatural amino acid residues. The V74I mutant of RNase HI has 2.1 K higher melting temperature and 0.6 kcal/mol larger unfolding free energy than the wild type [16]. Crystal structures of the wild type and V74I mutant of RNase HI have also been determined [16, 17]. These X-ray crystallographic studies showed that the side chain group of Val74 faces a cavity in the hydrophobic core and the C β atom of Ile74 fills the cavity. The structure around Ile74 of the V74I mutant does not significantly deviate from that of the wild type. The only significant difference between the wild type and the V74I mutant structures is the existence of the Ile74 side chain methyl group. Why is the V74I RNase HI mutant stabilized relative to the wild type by introducing a methyl group into the interior of the enzyme? Such a stabilization could arise from an increase in favorable packing interactions inside the mutant and/or by a loss of the solvation energy in the mutant denatured state due to the creation of an extra methyl group exposed to water [13]. Thermodynamics experiments cannot determine which mechanism is dominant, because they can only determine the free energy difference between the native and denatured states of a protein and not the free energy difference between a wild type and its mutant in the same state.

In recent years, several theoretical studies of protein stability have been made using free energy perturbation calculations combined with molecular dynamics (MD) simulations [18–23]. In this methodology, a protein's amino acid is mutated by gradually changing its force-field parameters during an MD simulation. The free energy change due to the mutation can then be evaluated. This theoretical approach can provide the free energy change due to the mutation in both the native and denatured states. Furthermore, the dominant factors causing the stability change can be analyzed by searching for leading terms in the free energy changes [18, 23]. However, the reliability of the results obtained by such approach depends on the level of approximations used in the simulations [25]. The studies reported previously used the following approximations: most of the protein atoms are fixed to their initial positions, only a part of the protein is solvated, and long-range Coulomb interactions are neglected by using the cutoff approximation. Yun-yu *et al.* have demonstrated that thermodynamic quantities obtained depend significantly on the approximations (such as the cutoff radius) under which the simulations are performed [20].

Our purpose in the present study is to clarify the stabilization mechanism for the Val74→Ile mutant of RNase HI relative to the wild type using the free energy perturbation method based on MD simulations. In order to obtain reliable and objective results, MD simulations based on more sophisticated methodologies were carried out [26, 34]. That is, no artificial constraint was applied on the protein structure, the protein was immersed in a sphere of water and fully solvated, and all long-range Coulomb interactions were taken into account. These conditions are essential to prevent the protein structure from undergoing artificial deformations

during the MD trajectories [26]. All MD simulations were carried out using the program package COSMOS90 based on the particle-particle and particle-cell (PPPC) approximation [27], which makes it possible to calculate long-range Coulomb interactions efficiently without sacrificing accuracy.

Subsequently, to estimate the hysteresis error in our simulations, we carried out a further simulation of the reverse mutation. Using the trajectories obtained from the MD simulations, the free energy changes of the native and denatured states were evaluated by the acceptance ratio method (ARM) [31,32]. A mechanism for the stabilization of the mutant relative to the wild type was revealed by finding leading contributions to the free energy changes.

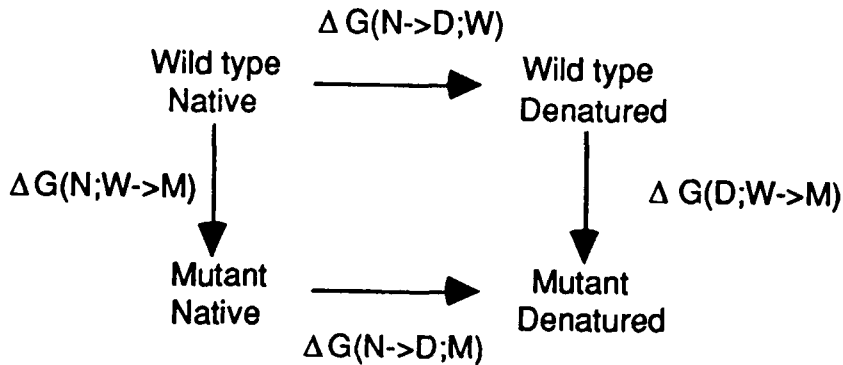
2 CALCULATION METHODS

2.1 Unfolding free energy difference $\Delta\Delta G(N \rightarrow D; W \rightarrow M)$

The stability change caused by the mutation is defined by the unfolding free energy difference between the wild type and the mutant, $\Delta\Delta G(N \rightarrow D; W \rightarrow M)$.

$$\Delta\Delta G(N \rightarrow D; W \rightarrow M) = \Delta G(N \rightarrow D; M) - \Delta G(N \rightarrow D; W) \quad (1)$$

where $\Delta G(N \rightarrow D; W)$ and $\Delta G(N \rightarrow D; M)$ denote the free energy changes by unfolding from the native (N) to the denatured (D) state for the wild type (W) and the mutant (M), respectively. Thermodynamic experiments such as differential scanning calorimetry measure directly $\Delta G(N \rightarrow D; W)$ and $\Delta G(N \rightarrow D; M)$. On the other hand, free energy calculations based on MD simulations mutating the wild type to the mutant determine free energy changes due to the mutation in the native and denatured states, $\Delta G(N; W \rightarrow M)$ and $\Delta G(D; W \rightarrow M)$. These free energy changes are related to $\Delta G(N \rightarrow D; M)$, $\Delta G(N \rightarrow D; W)$, and $\Delta\Delta G(N \rightarrow D; W \rightarrow M)$ by the following thermodynamic cycle.



Therefore, the unfolding free energy difference between the wild type and the mutant $\Delta\Delta G(N \rightarrow D; W \rightarrow M)$ can be also evaluated from $\Delta G(D; W \rightarrow M)$ and $\Delta G(N; W \rightarrow M)$ according to the following equation [34].

$$\Delta\Delta G(N \rightarrow D; W \rightarrow M) = \Delta G(D; W \rightarrow M) - \Delta G(N; W \rightarrow M) \quad (2)$$

2.2 Systems for the native and denatured states

The starting structure of the native protein was prepared by immersing the V74I mutant of *Escherichia coli* RNase HI with crystal waters [16] into a water sphere with the radius of 33 Å and the density of 1.0 g/cm³. The sphere radius of 33 Å was such that the minimum distance of any protein atom from the wall of the sphere was about 8 Å. The denatured state was assumed to be represented by the five amino acid segment centered at the residue 74 (Ace-Gln-Tyr-Ile(Val)-Arg-Gln-NMe), because there is no unique choice for the denatured state [18–23]. The starting structure of the denatured state was prepared by immersing the segment with the extended conformation into a water sphere of radius 21 Å. Water molecules colliding with the solute atoms or the crystal waters were removed. The native state system consists of 2474 protein atoms and 4049 water molecules. For the denatured state, the system consists of 110 solute atoms and 1083 water molecules.

2.3 Molecular dynamics simulations

The AMBER all-atom type force-field parameters [28] were used for the solute molecules, and the SPC model [29] for the water molecules. The force field parameters of the protein were prepared using AMBER3.0 Rev.A [30]. The MD simulations were carried out for both systems with long-range Coulomb interactions included by using the program COSMOS90 based on the PPPC approximation [27]. Accuracy parameters used in the PPPC approximation were the same as those in the previous study [26]. The reliability and accuracy of this method were demonstrated in those papers. All the simulations were performed at a temperature of 300 K with a time step of 0.5 fs. At first, water molecules surrounding the solutes were equilibrated by 10ps MD simulation with the positions of solute heavy atoms, and the centers-of-mass of the crystal waters, constrained. Next, the whole system was equilibrated during a 90 ps MD simulation without any constraints. All MD simulations for the computational mutations from Ile to Val were started from the equilibrated structure at 100 ps.

2.4 Procedures for the computational mutation

The computational mutation from Ile to Val was carried out for the native state and denatured state by the following procedure. In order to calculate $\Delta G(N; W \rightarrow M)$ and $\Delta G(D; W \rightarrow M)$ for the Ile \rightarrow Val mutation, the force field parameters of the side chain atoms of Ile were gradually transformed into those of Val over the following 4 subprocesses in a total of 20 stages. Only one force field was changed in each subprocess.

Subprocess 1 (The 1st stage)

Atomic charges of Ile are changed linearly to those of Val.

Subprocess 2 (The 2nd ~ 11th stage)

The force field parameters of the vdW interactions are linearly changed to those of Val.

Subprocess 3 (The 12th stage)

The force field parameters of the bond angles (*i.e.* equilibrium angle and force constant) are linearly changed to those of Val.

Subprocess 4 (The 13th ~ 20th stage)

The force field parameters of the bonds (*i.e.* equilibrium distance and force constant) are linearly changed to those of Val.

The force field parameters of the torsion angles are identical in Val and Ile. By the last stage of the subprocess 4, all the force field parameters have been changed into those of Val. Each stage consists of a 10ps MD simulation, *i.e.*, 5ps for equilibration and 5 ps for data collection. In order to estimate the hysteresis error in the present simulations, a further simulation of the reverse mutation, from Val to Ile, was carried out in the same manner. The first stage of the reverse mutation was begun from the final stage of the forward mutation, and the force field parameters were changed according to the reverse order of the forward mutation, *i.e.*, in the order of bond, angle, vdW and then electrostatic parameters.

2.5 Free energy calculations

The free energy changes of the native and denatured states due to the mutation were obtained by summing the free energy differences between two sequential stages i and $i + 1$, *i.e.*,

$$\Delta G(N; W \rightarrow M) = \sum_i \Delta G(N; i \rightarrow i + 1) \quad (3)$$

$$\Delta G(D; W \rightarrow M) = \sum_i \Delta G(D; i \rightarrow i + 1) \quad (4)$$

The free energy difference between two sequential stages $\Delta G(N \text{ or } D; i \rightarrow i + 1)$ was calculated by the acceptance ratio method (ARM) [31, 32], as follows.

$$\Delta G(N \text{ or } D; i \rightarrow i + 1) = \frac{C}{\beta} - \frac{1}{\beta} \log \left(\frac{n_{i+1}}{n_i} \right) \quad (5)$$

$$n_i \left\langle \frac{1}{e^{\beta(U_{i+1} - U_i) - C} + 1} \right\rangle_i = n_{i+1} \left\langle \frac{1}{e^{\beta(U_i - U_{i+1}) + C} + 1} \right\rangle_{i+1} \quad (6)$$

where U_i and U_{i+1} denote the potential energies calculated for the force-field parameters of stage i and $i + 1$, respectively. $\langle \rangle_i$ means sample average over configurations in stage i , and n_i denotes the number of sample configurations of stage i . The value of the shift constant C that satisfies Eq. (6) is determined numerically by evaluating the left and right sides of this equation for several values of C [31]. Since ARM utilizes samples from both ensembles, ARM can evaluate a free energy difference between the two ensembles more efficiently than the conventional free energy perturbation method (FEP) which uses samples from only one ensemble.

Since only one force-field parameter is changed in each subprocess, the free energy obtained from the subprocess represents the respective energy component in the free energy change due to the mutation. Values of the free energy components in principle depend on the order changing the force field parameters, *i.e.* the order of subprocesses [24]. That is, the free energy obtained from the subprocess 2 is the free energy change

caused by eliminating the C_β methyl group whose atomic charges are zero. On the other hand, contributions from different atom groups α and β surrounding the residue 74 were estimated by using the conventional free energy component analysis, *i.e.*, evaluating the free energy from Eq. (6), while $U_{i+1} - U_i$ of the left side and $U_i - U_{i+1}$ in the right side were evaluated for the respective atom groups α and β . This analysis gives the meaningful free energy contributions from the atomic groups, when $\{U_{i+1} - U_i\}_\alpha$ and $\{U_{i+1} - U_i\}_\beta$ do not largely correlate each other [35]. This condition was ensured to be satisfied in this study, as described in the table caption.

3 RESULTS AND DISCUSSION

3.1 Free energy changes due to the mutation Val74 → Ile

Free energy changes of the native state and denatured state due to the mutation Val74 → Ile were shown in Table 1. The mutation from Val to Ile caused free energy changes of 1.60 ± 0.19 kcal/mol for the native state and 2.25 ± 0.00 kcal/mol for the denatured state. Then, the unfolding free energy difference $\Delta\Delta G$ between the wild type protein and the V74I mutant protein was 0.66 ± 0.19 kcal/mol. The value of the calculated $\Delta\Delta G$ is in good agreement with the experimental data, 0.6 kcal/mol [16], as shown in Table 1. The deviation ± 0.19 denotes the hysteresis error, *i.e.* the deviation of the free energy values of the forward and reverse mutations from their average value but not a standard deviation within a given simulation. This hysteresis error is very small compared with those of previous studies [19, 20, 23]. The previous studies of the stability of T4 lysozyme mutants by Dang *et al.* demonstrated that additional position restraints for protein atoms in MD simulations significantly decreased the hysteresis error from ± 1.1 to 0.35 [18, 19]. Their results suggest that a large hysteresis error can be caused by artificial deformations of the protein structure. The present methodology is known to reduce such structural artifacts [26].

The root mean square deviation (RMSD) from the initial X-ray structure was plotted in Figure 1 for the residue 74 and the surrounding 6 residues in Figure 2 during the

Table 1 Free energy changes of the native (N) and denatured (D) states due to the Val → Ile mutation, $\Delta G(N; W \rightarrow M)$ and $\Delta G(D; W \rightarrow M)$, and the unfolding free energy difference between the wild type (W) and mutant (M), $\Delta\Delta G(N \rightarrow D; W \rightarrow M)$, in kcal/mol.

	$\Delta G(N; W \rightarrow M)$	$\Delta G(D; W \rightarrow M)$	$\Delta\Delta G(N \rightarrow D; W \rightarrow M)$
Total	1.60 ± 0.19	2.25 ± 0.00	0.66 ± 0.19
Contribution		Experiment	0.6^a
vdW ^b	0.25 ± 0.20	1.10 ± 0.03	0.85 ± 0.21
Electrostatic	0.03 ± 0.02	0.01 ± 0.06	-0.02 ± 0.06
Internal ^c	1.32 ± 0.00	1.13 ± 0.10	-0.18 ± 0.10

^a Reference [16].

^b The correlation coefficient between the vdW and internal components is smaller than 0.1.

^c Contributions from the bond, angle, 1–4 nonbond, and 1–5 nonbond in the side chain atoms of the residue 74 except for the C_β methine group.

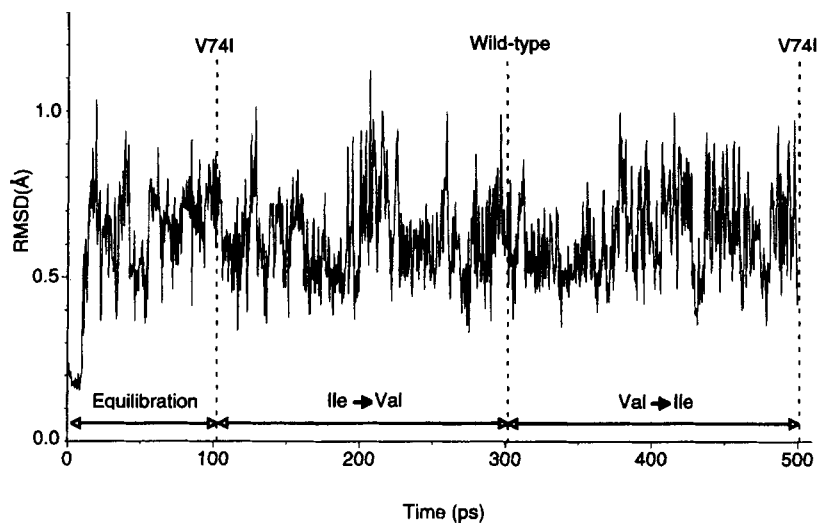


Figure 1 Root mean square deviation (RMSD) for heavy atoms of the 7 residues in Figure 2 from the X-ray structure during the equilibration (0–100ps), forward mutation (100–300ps), and reverse mutation (300–500ps).

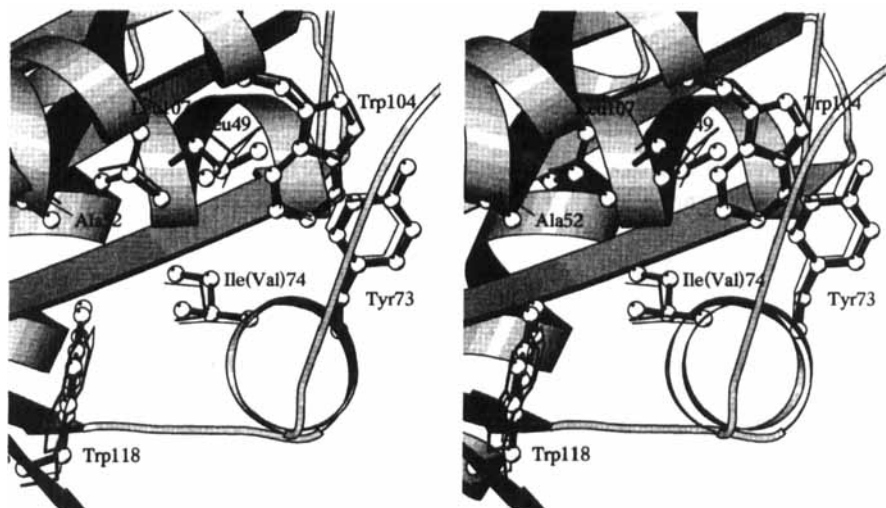


Figure 2 Three-dimensional structure of the residue 74 and 6 residues surrounding it. The ball-and-stick, thick line, and thin line denote the structures after the equilibration (A), forward mutation (B), and reverse mutation (C). These structures A, B, and C were fitted by the least-square method for the heavy atoms of the 7 residues. RMS deviations between A and B, B and C, and C and A are 0.3, 0.4, and 0.5Å, respectively. This figure was drawn by MolScript [33].

equilibration and the round trip mutation. The Figure 1 shows that the structure around the residue 74 fluctuates around a stable structure which is close to the X-ray structure during the forward and reverse mutation processes. The 3-dimensional structure averaged over 5ps was drawn around the residue 74 for the time after the

equilibration, forward mutation, and reverse mutation by the ball and stick, thick line, and thin line, respectively. This figure clearly shows that the side chains have almost the same structure within the thermal fluctuation (about 0.5Å) during the simulations. It was found that the present MD simulations without the truncation of Coulomb interactions suppress the hysteresis error and prevent artificial structural deformations of the protein.

3.2 Stabilization mechanism of the Val74 → Ile mutant

Which mechanism is dominant as a stabilization mechanism of the Val74 → Ile mutant: an increase in favorable packing interactions due to the C_δ methyl group inserted into the native protein, or a loss of the hydration energy due to the extra methyl group exposed to water in the denatured state? The relatively large $\Delta G(D; W \rightarrow M)$ ($= 2.25$ kcal/mol) compared with $\Delta G(N; W \rightarrow M)$ ($= 1.60$ kcal/mol) shown in Table 1 suggests that the latter mechanism is dominant. To answer that question clearly, the free energy changes $\Delta G(N; W \rightarrow M)$, $\Delta G(D; W \rightarrow M)$, and $\Delta\Delta G$ were decomposed into vdW, electrostatic, and internal energy contributions, as shown in Table 1.

The component of vdW interaction was small (0.25 kcal/mol) for $\Delta G(N; W \rightarrow M)$, relatively large (1.10 kcal/mol) for $\Delta G(D; W \rightarrow M)$. Then, the vdW component in $\Delta\Delta G$ was 0.85 kcal/mol. In contrast, the component of electrostatic interaction in $\Delta G(N; W \rightarrow M)$ and $\Delta G(D; W \rightarrow M)$ were nearly equal zero, because the changes in the atomic charges due to the mutation from Val to Ile are quite small. Then, the component of electrostatic interaction in $\Delta\Delta G$ was negligibly small -0.02 kcal/mol. The internal energy components were large and similar values 1.32 and 1.13 kcal/mol for $\Delta G(N; W \rightarrow M)$ and $\Delta G(D; W \rightarrow M)$, respectively. Since they are almost cancelled out each other, the internal energy component in $\Delta\Delta G$ is small (-0.18 kcal/mol). This cancellation suggests that the internal structures of Val and Ile are almost the same between the native and denatured proteins. Therefore, the stabilization of the V74I

Table 2 Contributions of the solvent and solute to the vdW free energy components, $\Delta G_{\text{vdW}}(N; W \rightarrow M)$, $\Delta G_{\text{vdW}}(D; W \rightarrow M)$, and $\Delta\Delta G_{\text{vdW}}(N \rightarrow D; W \rightarrow M)$ in Table 1.

	$\Delta G_{\text{vdW}}(N; W \rightarrow M)$	$\Delta G_{\text{vdW}}(D; W \rightarrow M)$	$\Delta\Delta G_{\text{vdW}}(N \rightarrow D; W \rightarrow M)$
Solvent ^a	-0.07 ± 0.01	0.73 ± 0.06	0.80 ± 0.06
Solute	0.32 ± 0.20	0.37 ± 0.03	0.05 ± 0.20
Residue ^b			
Val(Ile)74	0.47 ± 0.14	0.54 ± 0.12	0.07 ± 0.17
Leu49 ^c	0.89 ± 0.29	—	-0.89 ± 0.29
Ala52	-0.06 ± 0.01	—	0.06 ± 0.01
Tyr73	-0.19 ± 0.02	-0.09 ± 0.12	0.19 ± 0.12
Trp104	-0.20 ± 0.04	—	0.20 ± 0.04
Leu107	-0.12 ± 0.03	—	0.12 ± 0.03
Trp118	-0.06 ± 0.00	—	0.06 ± 0.00
Others	-0.41 ± 0.23	-0.08 ± 0.06	0.33 ± 0.24

^a The correlation coefficient between the solvent and solute contributions is smaller than 0.1.

^b Whose contribution is larger than 0.05.

^c The correlation coefficients between the contributions from Leu49 and other residues are smaller than 0.3.

mutant was found to be mainly caused by the unfavorable vdW interactions in the denatured state.

Furthermore, contributions from the solute and solvent to the vdW components in $\Delta G(N; W \rightarrow M)$, $\Delta G(D; W \rightarrow M)$, and $\Delta \Delta G$ [abbreviated by $\Delta G_{\text{vdW}}(N; W \rightarrow M)$, $\Delta G_{\text{vdW}}(D; W \rightarrow M)$, and $\Delta \Delta G_{\text{vdW}}$] were estimated. The results were shown in Table 2. The solvent contribution was -0.07 for $\Delta G_{\text{vdW}}(N; W \rightarrow M)$, 0.73 for $\Delta G_{\text{vdW}}(D; W \rightarrow M)$, and then 0.80 for $\Delta \Delta G_{\text{vdW}}$. The small solvent contribution to $\Delta G_{\text{vdW}}(N; W \rightarrow M)$ is consistent with the fact that the side chain atoms of Val (and Ile) 74 is completely buried inside the native protein. On the other hand, the solvent contribution to $\Delta G_{\text{vdW}}(D; W \rightarrow M)$ is relatively large, because the side chain atoms is exposed into solvent in the denatured state. This solvent contribution increasing the denatured state free energy can be explained as a loss of the solvation energy caused by the C_δ methyl group created in water. On the other hand, the solute contributions to $\Delta G_{\text{vdW}}(N; W \rightarrow M)$ and $\Delta G_{\text{vdW}}(D; W \rightarrow M)$ are almost the same (0.32 and 0.37) and are cancelled out each other in $\Delta \Delta G_{\text{vdW}}$. The positive contribution to $\Delta G_{\text{vdW}}(N; W \rightarrow M)$ (0.32) means that the vdW interactions of the C_δ methyl group inside the protein do not stabilize the cavity-filling mutant V74I. Therefore, the stabilization of the V74I mutant was found to be caused by the loss of the hydration energy in the denatured state but not the favorable packing interactions in the native protein.

In order to clarify the reason why the C_δ methyl group of Ile74 does not interact favorably inside the protein, the contributions from the surrounding 6 residues in Figure 2 were also listed in Table 2. All the residues except for Leu49 have negative values as contributions to $\Delta G_{\text{vdW}}(N; W \rightarrow M)$ and contribute to the stabilization of the V74I mutant. In contrast, the Leu49 has a positive value (0.89) and contributes to the destabilization of the native state. These results suggest that the cavity size between the Val74 and Leu49 side chains is too small to insert a methyl group into it without unfavorable vdW repulsion. Since the unfavorable vdW interactions with the Leu49 offset the favorable vdW interactions with the other surrounding residues, the insertion of the C_δ methyl group into the cavity can not stabilize the mutant native structure.

4 CONCLUSION

The cavity-filling mutation stabilizes a protein generally by the two different mechanisms. One is an increase of favorable vdW interactions inside a protein; another is a loss of the hydration energy of the denatured state. The MD simulation/free energy calculation study of the RNase HI V74I mutant clarified that this mutant is stabilized thermally by the latter mechanism. The former mechanism does not stabilize the mutant because of the unfavorable interactions with Leu49.

Acknowledgements

We are grateful to Dr. Kohki Ishikawa for providing us the X-ray structure of V74I mutant and to Dr. Philip Jewsbury for his careful reading of this manuscript.

References

- [1] K. A. Dill, "Dominant Forces in Protein Folding", *Biochemistry*, **29**, 7133 (1990).
- [2] A. E. Eriksson, W. A. Baase, X.-J. Zhang, D. W. Heinz, M. Blaber, E. P. Baldwin and B. W. Matthews, "Response of a Protein Structure to Cavity-Creating Mutations and Its Relation to the Hydrophobic Effect", *Science*, **255**, 178 (1992).
- [3] D. Shortle, W. E. Stites and A. K. Meeker, "Contributions of the Large Hydrophobic Amino Acids to the Stability of Staphylococcal Nuclease", *Biochemistry*, **29**, 8033 (1990).
- [4] J. T. J. Kellis, K. Nyberg, D. Sali and A. R. Fersht, "Contribution of hydrophobic interactions to protein stability", *Nature*, **333**, 784 (1988).
- [5] J. T. J. Kellis, K. Nyberg and A. R. Fersht, "Energetics of Complementary Side-Chain packing in a Protein Hydrophobic Core", *Biochemistry*, **28**, 4914 (1989).
- [6] W. S. Sandberg and T. C. Terwilliger, "Energetic of repacking a protein interior", *Proc. Natl. Acad. Sci. USA*, **88**, 1706 (1991).
- [7] S. Dao-pin, T. Alber, W. A. Baase, J. A. Wozniak and B. W. Matthews, "Structural and Thermodynamic Analysis of the Packing of Two α -Helices in Bacteriophage T4 Lysozyme", *J. Mol. Biol.*, **221**, 647 (1991).
- [8] M. Matsumura, W. J. Backtel and B. W. Matthews, "Hydrophobic stabilization in T4 lysozyme determined directly by multiple substitutions of Ile 3", *Nature*, **334**, 406 (1988).
- [9] M. Matsumura, J. A. Wozniak, S. Dao-pin and B. W. Matthews, "Structural studies of mutants of T4 lysozyme that alter hydrophobic stabilization", *J. Biol. Chem.*, **264**, 16059 (1989).
- [10] J. H. Hurley, W. A. Baase and B. W. Matthews, "Design and structural analysis of alternative hydrophobic core packing arrangements in bacteriophage T4 lysozyme", *J. Mol. Biol.*, **224**, 1143 (1992).
- [11] K. Yutani, K. Ogasahara, T. Tsujita and Y. Sugino, "Dependence of conformational stability on hydrophobicity of the amino acid residue in a series of variant proteins substituted at a unique position of tryptophan synthase α -subunit", *Proc. Natl. Acad. Sci. USA*, **84**, 4441 (1987).
- [12] W. A. Lim and R. T. Sauer, "The role of internal packing interactions in determining the structure and stability of a protein", *J. Mol. Biol.*, **219**, 359 (1991).
- [13] W. S. Sandberg and T. C. Terwilliger, "Influence of interior packing and hydrophobicity on the stability of a protein", *Science*, **245**, 54 (1989).
- [14] M. Karpusas, W. A. Baase, M. Matsumura and B. W. Matthews, "Hydrophobic packing in T4 lysozyme probed by cavity-filling mutants", *Proc. Natl. Acad. Sci. USA*, **86**, 8237 (1989).
- [15] V. G. H. Eijsink, B. W. Dijkstra, G. Vriend, J. R. van der Zee, O. R. Veltman, B. van der Vinne, B. van den Burg, S. Kempe and G. Venema, "The effect of cavity-filling mutations on the thermostability of *Bacillus stearothermophilus* neutral protease", *Protein Eng.*, **5**, 421 (1992).
- [16] K. Ishikawa, H. Nakamura, K. Morikawa and S. Kanaya, "Stabilization of *Escherichia coli* Ribonuclease HI by Cavity-Filling Mutations within a Hydrophobic Core", *Biochemistry*, **32**, 6171 (1993).
- [17] K. Katayanagi, M. Miyazawa, M. Matsushima, M. Ishikawa, S. Kanaya, H. Nakamura, M. Ikehara, T. Matsuzaki and K. Morikawa, "Structural Details of Ribonuclease H from *Escherichia coli* as Refined to an Atomic Resolution", *J. Mol. Biol.*, **223**, 1029 (1992).
- [18] L. X. Dang and P. A. Kollman, "Free energy calculations on protein stability: The Thr157 \rightarrow Ala157 mutation of T4 Lysozyme", "Proteins Structure, Dynamics and Design" edited by V. Renugopalakrishnam, P. R. Carey, I. C. P. Smith, S. G. Huang and A. C. Storer, ESCOM, Leiden (1991).
- [19] L. X. Dang, K. M. J. Merz and P. A. Kollman, "Free Energy Calculations on Protein Stability: Thr-157 \rightarrow Val-157 Mutation of T4 Lysozyme", *J. Am. Chem. Soc.*, **111**, 8505 (1989).
- [20] S. Yun-yu, A. E. Mark, W. Cun-xin, H. Fuhua, H. J. C. Berendsen and W. F. van Gunsteren, "Can the stability of protein mutants be predicted by free energy calculations?", *Protein Engineering*, **6**, 289 (1993).
- [21] B. Tidor and M. Karplus, "Simulation Analysis of the Stability Mutant R96H of T4 Lysozyme", *Biochemistry*, **30**, 3217 (1991).
- [22] S. F. Sneddon and D. J. Tobias, "The Role of Packing Interactions in Stabilizing Folded Proteins", *Biochemistry*, **31**, 2842 (1992).
- [23] M. Prevost, S. J. Wodak, B. Tidor and M. Karplus, "Contribution of the hydrophobic effect to protein stability: Analysis based on simulations of the Ile-96 \rightarrow Ala mutation in barnase", *Proc. Natl. Acad. Sci. USA*, **88**, 10880 (1991).

- [24] S. Boresch, G. Archontis and M. Karplus, "Free Energy Simulations: The Meaning of the Individual Contributions From a Component Analysis", *PROTEINS: Structure, Function, and Genetics*, **20**, 25 (1994).
- [25] W. F. van Gunsteren and A. E. Mark, "On the interpretation of biochemical data by molecular dynamics computer simulation", *Eur. J. Biochem.*, **204**, 947 (1992).
- [26] M. Saito, "Molecular dynamics simulations of proteins in solution: Artifacts caused by the cutoff approximation", *J. Chem. Phys.*, **101**, 4055 (1994).
- [27] M. Saito, "Molecular Dynamics Simulations of Proteins in Water without the Truncation of Long-range Coulomb Interactions", *Molecular Simulation*, **8**, 321 (1992).
- [28] S. J. Weiner, P. A. Kollman, D. A. Case, U. C. Singh, C. Ghio, G. Alagona, S. J. Profeta and P. Weiner, "A New Force Field for Molecular Mechanical Simulation of Nucleic Acids and Proteins", *J. Am. Chem. Soc.*, **106**, 765 (1984).
- [29] H. J. C. Berendsen, J. P. M. Postma, W. F. von Gunsteren and J. Hermans, "Interaction models for water in relation to protein hydration", in *Intermolecular Forces*, B. Pullman, ed., Reidel, Dordrecht, 1981, p. 331.
- [30] G. Seibel, U. C. Singh, P. K. Weiner, J. Caldwell and P. A. Kollman, *AMBER 3.0 Rev. A* (University of California, San Francisco, CA) (1989).
- [31] M. Saito and H. Nakamura, "Hydration Free Energy Calculations by the Acceptance Ratio Method", *J. Comp. Chem.*, **11**, 76 (1990).
- [32] C. H. Bennett, "Efficient Estimation of Free Energy Differences from Monte Carlo Data", *J. Comp. Phys.*, **22**, 245 (1976).
- [33] P. Kraulis, "MolScript, a program to produce both detailed and schematic plots of protein structures", *J. Appl. Crystallogr.*, **24**, 946 (1991).
- [34] M. Saito and R. Tanimura, "Relative melting temperatures of RNase HI mutant proteins from MD simulation / free energy calculations", *Chem. Phys. Letters*, **236**, 156 (1995).
- [35] P. E. Smith and W. F. van Gunsteren, "When are free energy components meaningful? ", *J. Phys. Chem.*, **98**, 13735 (1994).